FY19 Progress of EBS International Collaborations

Spent Fuel and Waste Disposition

Prepared for
US Department of Energy
Spent Fuel and Waste Science and Technology

Edward N. Matteo, Thomas A. Dewers, Carlos Jové-Colón, and Teklu Hadgu,
Sandia National Laboratories

C. Gruber, M. Steen, K. Brown, R. Delapp, L. Brown, D. Kosson,
Vanderbilt University

J.C.L. Meeussen,
NRG, Petten, The Netherlands

August 30, 2019
M4SF-19SN010308082
SAND2019-10787 R

SUMMARY

The SNL EBS International activities were focused on two main collaborative efforts for FY19 – 1) Developing analytical tools to study and better understand multi-phase flow and coupled-process physics in engineered barrier materials and at the interface between EBS materials and host media, and 2) Benchmarking of reactive transport codes (inclduing PFLOTRAN) used for chemcial evolution of cementitious EBS components. Topic 1 is being studied as part of the SKB EBS Task Force, while Topic 2 is being pursued as a collaboration with researchers from Vanderbilt University and NRG in the the Netherlands.

This page is intentionally left blank.

ACKNOWLEDGEMENTS

Sandia National Laboratories is a multimission laboratory managed and operated by National Technology and Engineering Solutions of Sandia LLC, a wholly owned subsidiary of Honeywell International Inc. for the U.S. Department of Energy's National Nuclear Security Administration under contract DE-NA0003525.

This page is intentionally left blank.

CONTENTS

This page is intentionally left blank.

LIST OF FIGURES

LIST OF TABLES

This page is intentionally left blank.

SPENT FUEL AND WASTE SCIENCE AND TECHNOLOGY/ENGINEERED BARRIER SYSTEM R&D

1. INTRODUCTION

This report summarizes the FY19 Progress in the Engineered Barrier System International Collaborations Work Package. The international collaborations work packages aim to leverage knowledge, expertise, and tools from the international nuclear waste community, as deemed relevant according to SFWST "roadmap" priorities. The EBS R&D work package scope encompasses aspects of repository design, as well as specific process models related to the technical basis and performance evaluation of EBS components. This report provides a summary for activity associated with FY19 Work Scope: Chapter 2 describes EBS WP participation in Task 9 of the SKB EBS task Force. Chapters 3 and 4 describe a complimentary set of international activities related to improving process models and simulation capabilities for cementitious materials.

2. SKB EBS Task Force Task 9: Updates on SNL Modeling Efforts

2.1 Summary

In FY2019 Sandia National Laboratories (SNL) is participating in the SKB EBS Task Force *Task 9*, the FEBEX (Full-scale Engineered Barriers Experiment in Crystalline Host Rock) full scale "in situ" test conducted during 18.4 years in the Grimsel URL (Switzerland) managed by NAGRA. The objectives of the task are to get better understanding of the THM behavior of the EBS during heating experiments. Sandia joined the task on its final year and thus the participation may be constrained by time limits. For Sandia the aim is to develop THM capabilities and to participate in an international project interacting with other teams.
Sandia is focusing on three main sub tasks, including:

- THM Modeling with Coupled CFD and Porous Flow: Effects of Barrier Gaps
- TH Modeling: Uncertainty Quantification and Parameter Estimation with PFLOTRAN
- THM Modeling of Gas Transport in Viscoelastoplastic Soft Materials

Preliminary results on these tasks were presented at the SKB Task Force meeting in Barcelona in May 2019. Updates on sub-tasks will be presented at the upcoming meeting in Baden Switzerland in November 2019. We anticipate completing these subtasks 1 and 2 by the end of the calendar year 2019, together with a final report. The subtask in bullet point #3 above will continue as advised and modified at the next SKB Task Force meeting.

2.1.1 Background for Sub-Tasks 1 and 2.

The FEBEX test area includes two electrical heaters emplaced in a tunnel surrounded by compacted bentonite blocks. The test area was closed with a concrete plug (see Figure 1.1). The work to be performed in the Task has been divided into 2 stages. This report is on Stage 1, which includes the operational period of the FEBEX experiment up to and including the dismantling of the first heater (5.0 years). For Task 9 each modeling team is to provide five types of results: (1) evolutions of heating power; (2) distributions and evolutions of relative humidity; (3) distributions and evolutions of temperature; (4) evolutions of total stresses; and (5) distributions after the first dismantling of dry density, water content and degree of saturation.

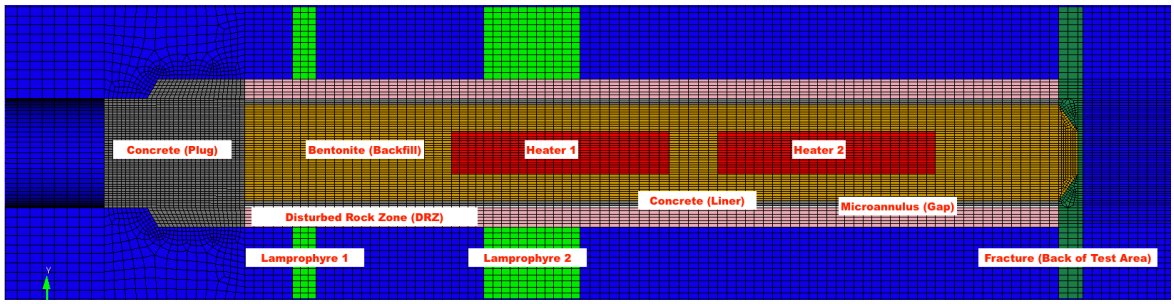

Figure 2-1. Symmetry plane of FEBEX simulation showing material domains.

2.1.2 3D THM Modeling with Coupled CFD and Porous Flow: Effects of Barrier Gaps

Work under this subtask involves developing a computational fluid dynamics (CFD) THM two-phase model for air and water in liquid and gas phases, to model transport in tunnel, gaps between the bentonite barrier and surrounding granite country rock, and cement plugs. We include a disturbed rock zone surrounding the tunnel excavation, lamprophyre dikes, and a fracture/shear zone intercepted at the rear of the tunnel. Our approach in this model is different from other Task 9 modeling. We employ a Forscheimer approximation including Navier-Stokes plus Brinkman corrections, which allows matching flux conditions between gaps and porous media, and a discontinuity in fluid pressure at bentonite boundaries. We use gas pressure and the molar density of water component as persistent variables for the compositional portion of the model, which allows continuous representation of the compositional model in the tunnel, cement, bentonite, and any open gaps during initial wetting up and dry out near heaters. Our focus is on gas flux and the influence of gaps and homogeneity in wetting up of the bentonite, and on the impact on thermal conductivity near the heaters. The 3D CFD model uses a tetrahedral mesh with the code COMSOL Multiphysics to solve the coupled TMH equations. The constitutive models for bentonite shrink/swell and thermal conductivity in particular have been validated against experimental data. Fully coupled simulations are being run on a Linux cluster at Sandia National Laboratories.

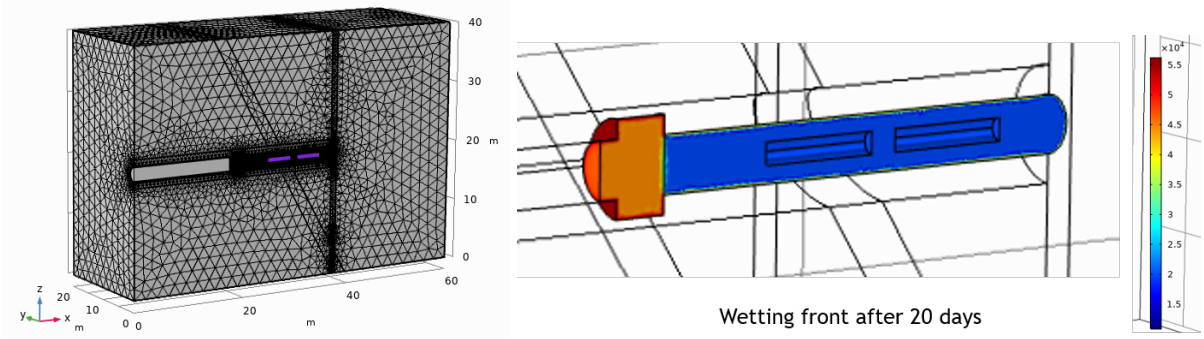

Figure 2-2. Simulation domain for Task 9 (heaters shown in purple) and results showing wetting front after twenty days in bentonite barrier and at cement plug-bentonite interface.

2.1.3 3D TH Modeling: Uncertainty Quantification and Parameter Estimation with PFLOTRAN

PFLOTRAN simulations of the FEBEX in-situ heater test is underway. At present the geometry of the test problem and meshing have been completed. Simulations of the preheating period before the heaters are turned on has started. That will be followed by simulation of heating with the two heaters on. The domain and mesh for PFLOTRAN were constructed based on the information given in Figure 1 and related project material. Only half of the geometry was modeled due to symmetry considerations. The resulting mesh includes 3,878,658 hexehedral elements and 3,970,770 nodes. The geometry of the mesh is shown in Figures 1 and 3.

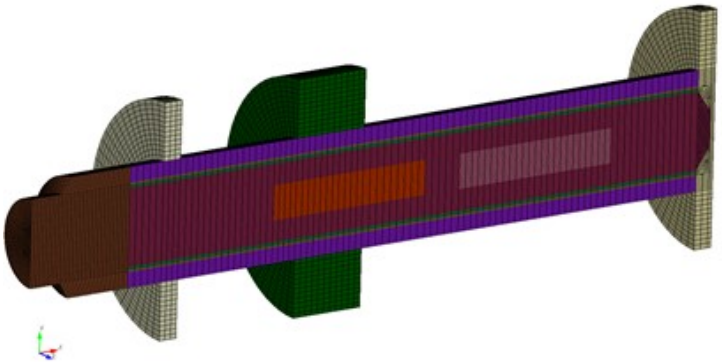

Figure 2-3. A 3-D view of the mesh showing use of symmetry to reduce computation burden.

The main focus of this sub-task is parameter estimation and uncertainty quantification made possible by coupling PFLOTRAN with the Sandia code DAKOTA. We are testing constitutive models for thermal conductivity of bentonite and fracture granite, using FEBEX temperature data as validation. The next step is to obtain a reasonable range of the relevant parameters and generate required output results using the coupled DAKOTA-PFLOTRAN software. The aim is also to extend the simulations beyond the dismantling of the first heater. Future work will also include participation in the next phase of the SKB EBS Task Force.

2.1.4 THM Modeling of Gas Transport In Viscoelastoplastic Soft Materials

For this subtask, we use a discrete interface phase field model to track wetting and drying fronts, and to examine the transition between viscous fingering and induced fracturing. Fractures in this case are developed by excess gas pressure, much like hydrofractures, and also by dry-out damge associated with bentonite shrinkage. The phase field method allows a continuum mechanics representation of interfaces and discontinuities, in which the interface advects, but also responds to thermodynamic principles of energy dissipation, and can capture quite complex dendritic fingering or branching fracture patterns. We use this methodology to both model injection of a Newtonian fluid into a viscoelastoplastic “soft” material, e.g. bentonite or mud, and create mosaics of damage zones associated with the dryout and shrinkage of the soft material. We have new experimental capability of a Deben mCT compression cell with humidity control, and plan to conduct bentonite dry-out experiments under compression to use for model validation. We started our modeling using COMSOL Multiphysics, but are examining the use of a Sandia-University of New Mexico open source code called GOMA, which is especially suited to computational issues surrounding the modeling of viscoelastic soft materials undergoing physico-chemical transitions.

3. Cement-Argillite Interaction Modeling – PFLOTRAN Benchmark

3.1 Introduction

Cement-clay interactions at the clay rock / cement interface play a key role the performance of seals and interactions with other barrier materials in deep geological nuclear waste repositories (Berner et al., 2013; Gaboreau et al., 2012; Kosakowski and Berner, 2013; Soler, 2012; Soler and Mader, 2010). The effects of porosity enhancement and reduction (i.e., clogging) due to mineral dissolution and precipitation have been the focus in various reactive-transport modeling efforts including benchmark test cases for computer code inter-comparisons (Marty et al., 2015; Xie et al., 2015). The main motivation behind these model / code assessments lies in the complex coupling of geochemical interactions (kinetic vs. transport controlled) and transport phenomena represented by reactive-transport models (Marty et al., 2015). Moreover, the extent to which these models capture relevant physico-chemical processes with enough realism and adequacy still needs to be examined and reconciled with the limited amount of available field and experimental data. The coupling of thermal-hydrological-chemical (THC) processes is a challenge on its own but the last two decades or so has brought key advances in the theoretical representation and hence computational simulation capabilities to represent these coupled phenomena.
The main purpose of this reactive-transport work is to evaluate a one-dimensional 1D benchmark model representation of cement / clay rock geochemical interactions by Marty et al. (2015) with diffusive transport using the computer code PFLOTRAN (Lichtner et al. 2013). This code has been selected as part of the core simulation platform for GDSA PA in the evaluation of disposal concepts (Mariner et al. 2015). Marty et al. (2015) compares the result of this benchmark excercise with a set of reactive transport codes (TOUGHREACT, PHREEQC, CRUNCH, HYTEC, ORCHESTRA, MIN3P-THCm) producing very similar results, even with differences on how these deal with transport processses.

A major feature of PFLOTRAN is its performance on massively parallel or high performance computing (HPC) platforms where efficient scalability becomes important for large coupled process problems that otherwise could present a computational limitation in other simulation codes. Parallelization is achieved through domain decomposition using the PETSc (Portable Extensible Toolkit for Scientific Computation) libraries. Lichtner et al. (2013) provides details on PFLOTRAN simulation capabilities, reactive-transport formulations, and geochemical treatment of mineral-fluid interactions.

3.1.1 Problem Description, Key Assumptions, and Parameter Variations

As mentioned previously, Marty et al (2015) evaluated this benchmark exercise with a set of reactive-transport computer codes programs, including TOUGHREACT, PHREEQC, CRUNCH, HYTEC, ORCHESTRA, and MIN3P. A model was developed based on the information set forth by Marty et al (2015), specifically for Case 2, which entails a 1D domain over 10,000 years. The modeled domain is 43 meters long, 3 meters of which is an OPC plug and the remainder is the argillite clay rock as depicted in **Figure 3-1**. The Cell widths are discretized to be consistent with the mesh refinement given by Marty et al. (2015). Cell height and depth, though not considered in the 1D calculations, is set to 1 meter for the meshed domain. It should be noted that Marty et al (2015) uses a radial grid discretization varying grid spacing with distance from the domain interface. That is, their grid spacings close to the cement / clay rock interface are more refined than those further away. In keeping with Marty et al (2015), the domain is assumed to be saturated in both regions. The starting pore solution compositions are listed in **Table 3-1**.

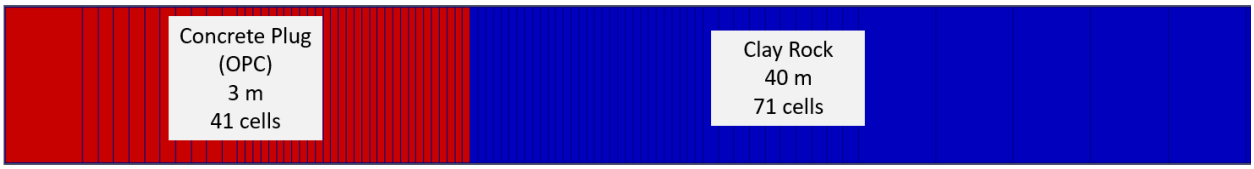

Figure 3-1. Design of the modeling domain. Not to-scale.

Table 3-1. Initial pore solution compositions

	Cement		Clay Rock	
Species	**Concentration (mol/L)**	**Remarks**	**Concentration (mol/L)**	**Remarks)**
Al+++	3.8E-05	-	8.4E-08	-
Fe++	4.6E-07	-	6.8E-05	-
H4SiO4(aq)	2.2E-05	-	1.8E-04	-
Sr++	1E-17	-	2.3E-04	-
K+	1.4E-01	-	5.1E-04	-
Mg++	1.5E-09	-	5.1E-03	-
Ca++	1.9E-03	-	7.6E-03	-
Na+	3.0E-02	-	4.0E-02	-
Cl-	4.1E-02	-	4.1E-02	-
SO4--	9.8E-04	-	1.1E-02	-
HCO3-	-13.1	Gaseous equilibrium with CO2 (bars)	3.8E-03	
O2(aq)	5.0E-15	-	5.0E-15	
H+	13.1	pH	7.0	pH

The problem is isothermal at 25ºC and modeled as diffusion-only with a diffusion coefficient of 1E-09 m^2/s applied to all chemical species. Porosities of 0.13 and 0.17 are adopted for the cement and clay rock, respectively. This results in effective diffusivities of 1.3174E-10 m^2/s for the cement and 1.718E-10 m^2/s for the argillite. No updates to permeability and porosity were considered nor any changes in porosity on chemical diffusion in the bulk porous media. It should be noted that Marty et al (2015) assumed porosity changes as a function of reaction progress and time. Ion exchange reactions were not considered in the simulations although PFLOTRAN has the capability to account for these as well as surface complexation. The minerals considered in the simulation are the same as those considered in Marty et al (2015). The authors provide mineral reactive surface areas (RSAs) for several species, though not all. Overall, RSAs of some phases are adjusted to fit concentration profile data. Volume fractions of the minerals in each region are listed in **Table 3-2**, which are scaled down relative to those from Marty et al (2015). The reason for the scale down is that volume fractions and porosities in Marty et al (2015) do not sum to unity. The correct input to PFLOTRAN requires that mineral volume fractions and porosities add up to unity.

Table 3-2. Volume fractions of minerals present in cement and argillite domains.

Cement	
Mineral	**Volume Fraction (initial)**
CSH(1.6)	0.175581
C3FH6	0.016574
Ettringite	0.032231
Hydrotalcite	0.006187
Monocarboaluminate	0.000764
Portlandite	0.048729
Calcite	0.588195
Clay Rock	
Mineral	**Volume Fraction (initial)**
Pyrite	0.008003
Calcite	0.203976
Celestite	0.008003
Chlorite(Cca-2)	0.016006
Dolomite	0.032012
Illite(IMt2)	0.264095
Microcline	0.024009
Montmorillonite(HcCa)	0.064023
Quartz(alpha)	0.200072
Siderite	0.008003

The THERMODDEM thermodynamic database (Blanc et al., 2012; Blanc et al., 2006) used in the calculations. Several logK values for mineral dissociation reactions in this database were updated to be consistent with those given in Marty et al. (2015) and are listed in **Table 3-2**. Mineral dissolution rate constants (RCs) are also provided by Marty et al (2015) for several mineral solids, though again not for all. These RCs were given for pH-basic, -acidic, and -neutral conditions, though applicable ranges are not specified. RCs are thus selected for the most relevant conditions, based on a neutral pH and calibrated to fit concentration data. pH-dependence of dissolution rates was not considered in this study. The RCs used can be found in **Table 3-3**.

Table 3-3. log K values and dissolution rate constants at 25 °C for considered minerals.

Mineral	Rate Constant (mol/m^2/sec)	logK (25 °C)
Amorphous silica	1.12E-14	-2.6997
Brucite	1.12E-15	17.1094
Clinoptilolite (Ca)	1.12E-15	-2.1071
CSH (1.6)	2.75E-12	28.0022
CSH (1.2)	1.12E-12	19.3013
CSH (0.8)	1.12E-12	11.0503
C3FH6	1.12E-12	72.3662
Ettringite	1.12E-12	56.9580
Ferrihydrite (2L)	1.12E-15	3.3991
Gypsum	1.3E-03	-4.6074
Hydrotalcite	1.12E-18	73.7346
$Fe(OH)_2$	1.12E-12	12.8494
Magnetite (am)	5.623E-11	14.5887
Monocarboaluminate	1.12E-12	80.5447
Mordenite B (Ca)	1.12E-15	-2.9185
Portlandite	5.04E-07	22.8094
Pyrite	2.884E-11	-23.5898
Pyrrhotite	1.12E-16	-3.6794
Saponite (Ca)	1.12E-15	28.07
Saponite (FeCa)	1E-18	26.5529
Straetlingite	1.12d-15	49.6567
Calcite	1.778E-06	1.8470
Celestite	2.2E-08	-6.6200
Chlorite (Cca-2)	1.0E-18	61.3152
Dolomite	1.1E-08	3.5328
Gibbsite (am)	1.12E-12	10.5743
Illite (IMt2)	5E-18	11.5220
Microcline	1.12E-14	0.0036
Montmorillonite (HcCa)	1.12E-17	7.28
Quartz (alpha)	5E-14	-3.7372
Siderite	1.12E-09	-0.2733

3.1.2 DAKOTA coupling

Sensitivity analyses and regressions for parameter evaluation are done using the DAKOTA software package (Adams et al., 2014), which allowed for multiple automated simulations done on high-performance computing Linux platforms. Specifically, DAKOTA's Hybrid Optimization Parallel Search

Package (HOPSPACK) is used. DAKOTA is set to optimize parameters based on minimization of an objective function that compares output values to values from Marty et al (2015). The objective function is the sum of squared differences between measured and predicted solute concentrations at a given time and domain location. Representative values from data trends in Marty et al (2015) are obtained via digitization of data depicted in the figures. DAKOTA makes use of the retrieved data to optimize pore solution concentration profiles at various observation points, by adjusting mineral RSAs, rate constants, and mineral volume fractions.

3.2 Results and Discussion

Figure 3-2 shows the predicted pH at 10,000 years as function of horizontal distance across the modeled domain. The interface between cement and clay rock is located at 3 m. Notice the good agreement between Marty et al (2015) and PFLOTRAN predictions. Sensitivity analysis simulations allowing for the presence and absence of ettringite in the cement region were conducted to evaluate the effect of this phase on certain solutes. **Figure 3-2** (top and lower panels) show the effect of ettringite on the pH profile where overall its presence produces results in better agreement with Marty et al (2015).

Trends for total Ca concentration profiles between Marty et al (2015) and this work shown in **Figure 3-3** are similar except for larger deviations in the ettringite-present case. Notice that these deviations tend to be large at the interface region whereas predictions within the bulk cement or clay rock tend to be in good agreement with Marty et al (2015), particularly in the ettringite-present case. This is also observed Figure 4 for the total dissolved Si profile where PFLOTRAN simulations do not predict large drops in concentration at the interface region compared to Marty et al (2015), but good agreement is observed within the bulk domains. The reason for these discrepancies at the interface is difficult to assess without key details about the grid discretization and the treatment of transport in the other codes used in Marty et al (2015). Further work is needed, for example, to conduct simulations allowing for porosity changes and feedbacks on permeability and diffusion particularly at the interface region.

Figures 3-5 and **3-6** shows total Mg and Na concentrations profiles for the two case scenarios, respectively. Both Mg concentration profiles show deviation in the cement region relative to Marty et al (2015) results but good agreement in the clay rock domain is observed for the ettringite-absent case. Mg concentration predictions at the interface show good agreement particularly in the ettringite-absent case. Marty et al (2015) specify an initial Na concentration in the cement. However, using this value as an initial input in our model resulted in an overestimate of the total Na concentration in the system noting that its concentration remains essentially unchanged by 10,000 years.

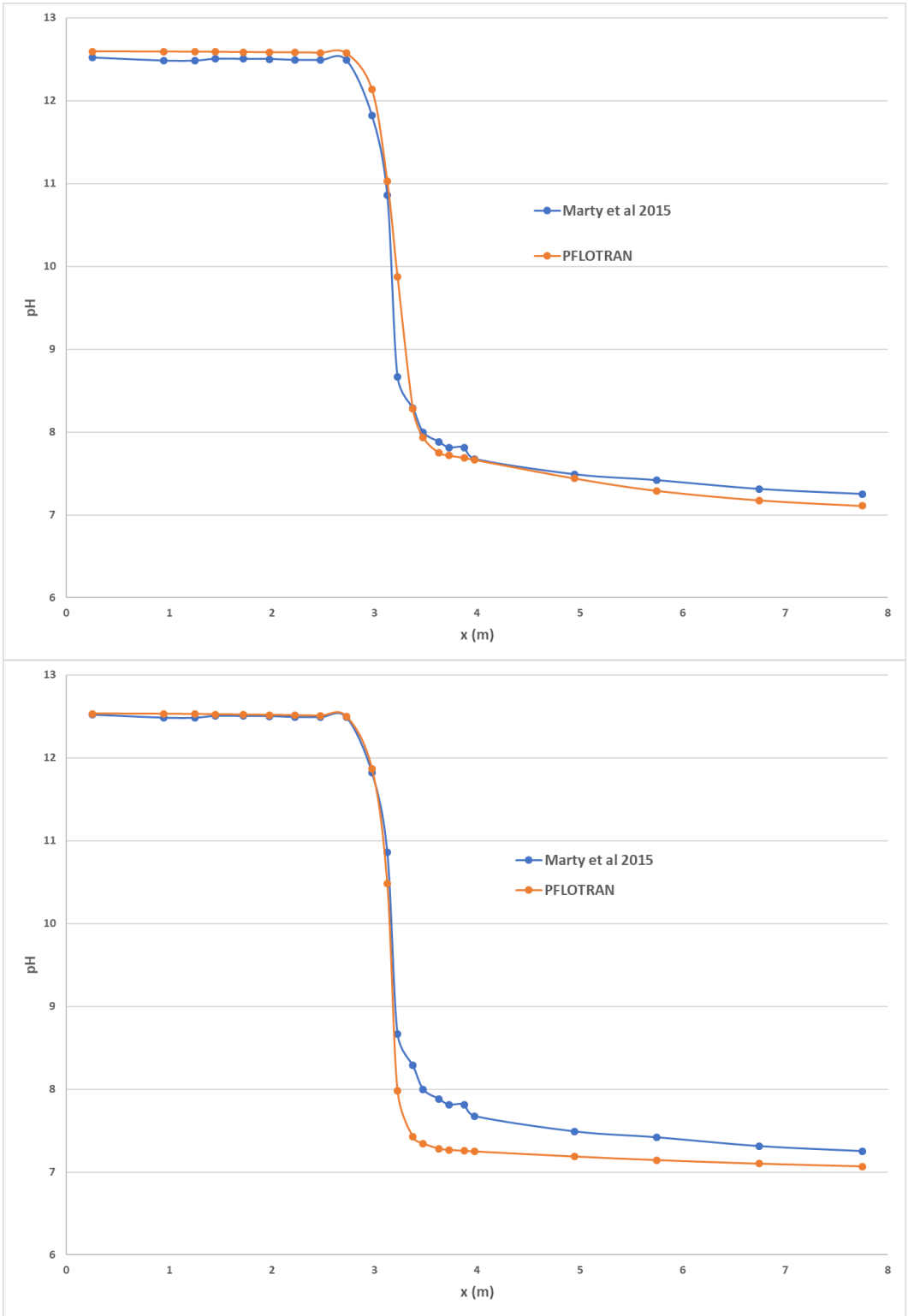

Figure 3-2. pH in the case with (above) and without (below) ettringite precipitation in the cement.

A very similar trend in the PFLOTRAN modeling results was otherwise observed, so the starting Na^+ concentration was decreased to obtain similar concertation at 10,000 years as shown in Figure 6. With this change, the resulting Na concentration is in very good agreement with that of Marty et al (2015) for both case scenarios.

Figures 3-7, 3-8, and 3-9 show the concentration profiles for total K, Al, and S. When compared to Marty et al (2015) model results, the K concentration profiles shown in Figure 7 indicate the most discrepant predictions from all the considered solutes both in the bulk domain and interface region. It is difficult to assess these deviations without further assessment of modeling details in the code simulations presented in Marty et al (2015). Sensitivity analyses were conducted for microcline rate constants and RSAs only to yield better agreement for solute concentrations the bulk clay rock. It should be noted that no K ion exchange reactions were considered in these simulations as oppose to Marty et al (2015). Figure 8 shows to Al concentration profile in good overall agreement with Marty et al (2015) results. An interesting feature of the PFLOTRAN Al profile close to the cement interface is the lack of sharp drops in concentration prior to an increase when closing into the clay rock domain. This trend is observed for both case scenarios. This trend somewhat similar to the Si concentration profile except the sharp drop in concentration occurs after its increase close to the cement interface. Figure 9 shows the concentration profiles for total S where the presence/absence of ettringite as a S-bearing phase in the cement has a clear effect on deviations from Marty et al (2015) results. The total S profile is in good agreement with the ettringite-present case with some shifting around the interface region. Some of the shifting of the profile in the interface region appears to be indicative of transport rate effects.

3.3 Conclusions

1D PFLOTRAN reactive transport simulations for a benchmark model problem of cement / clay rock domain (Marty et al., 2015) were conducted under isothermal conditions at 25°C for a period of 10,000 years. The simulations were conducted in the presence and absence of ettringite in the cement phase assemblage which has an influence on many solutes, particularly at the interface region. It should be noted that the choice of parameters and constrains in our simulations are somewhat different than those in Marty et al (2015) due to differences in the treatment of reactive transport and code run simplifications (e.g., no ion exchange, rate law). PFLOTRAN was coupled to the DAKOTA optimization software package to conduct parameter evaluation and sensitivities for mineral volume fraction, rate constants, and RSAs. Comparisons of resulting solute profiles at 10,000 years between PFLOTRAN and those given in Marty et al (2015) show, in general, good agreement of predicted trends for solute concentrations in the bulk cement and clay rock domain. However, deviations of these relative to the Marty et al (2015) results are observed at the interface region for several solutes. It is difficult to assess the reason for these deviations without detailed knowledge of the code simulations given in Marty et al (2015). This is important since most of the changes in the reactive dissolution front occur at the interface where sharp variations in solute concentrations control mineral precipitation/dissolution and their rates. At long time scales, large changes in porosity due to mineral dissolution/precipitation can have a strong influence on transport across the interface. More work is needed to refine mineral rate parameters and RSAs and conducting simulations to evaluate the effects of porosity and permeability changes on solute transport.

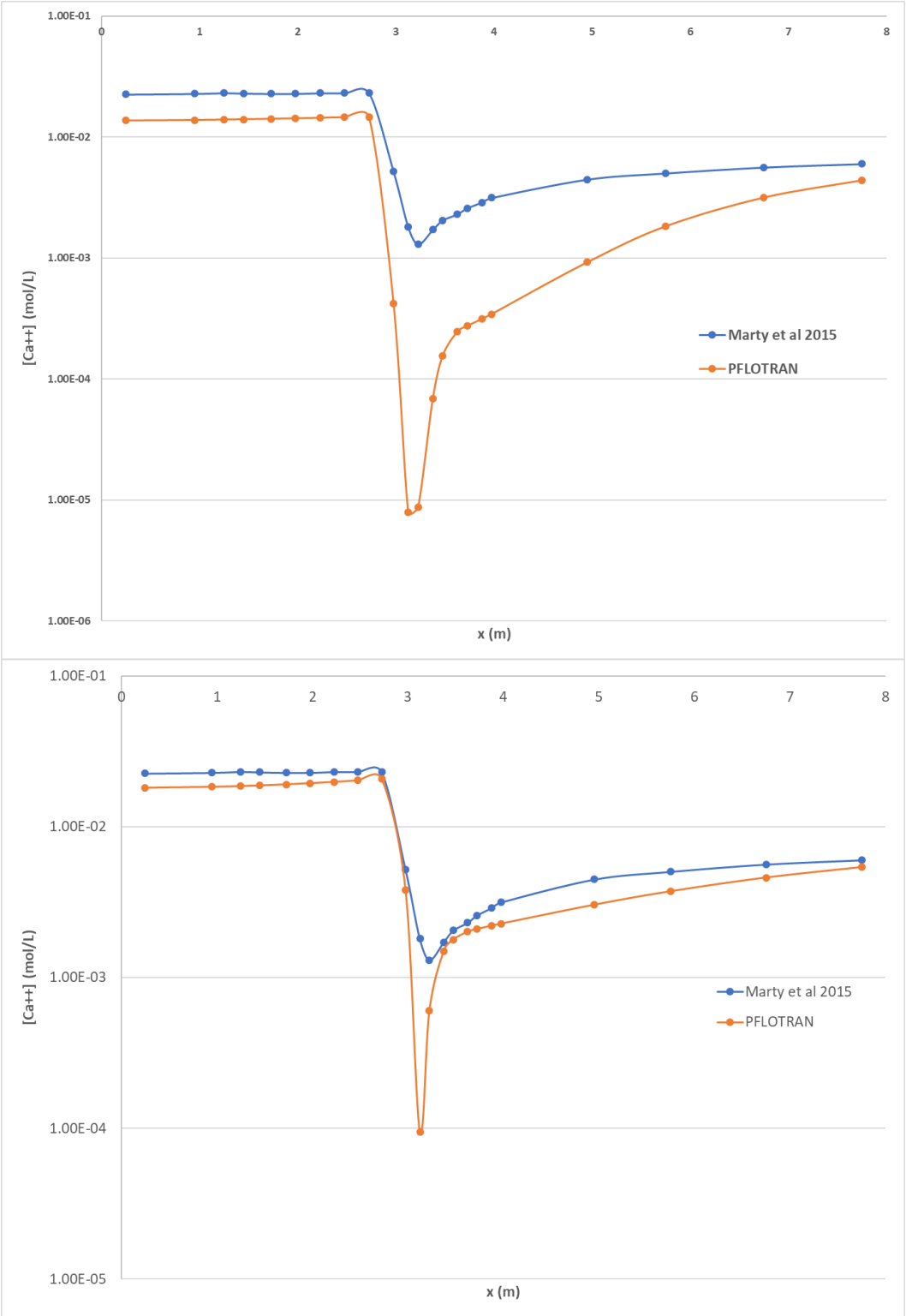

Figure 3-3. Ca^{++} concentration in the case with (above) and without (below) ettringite precipitation in the cement.

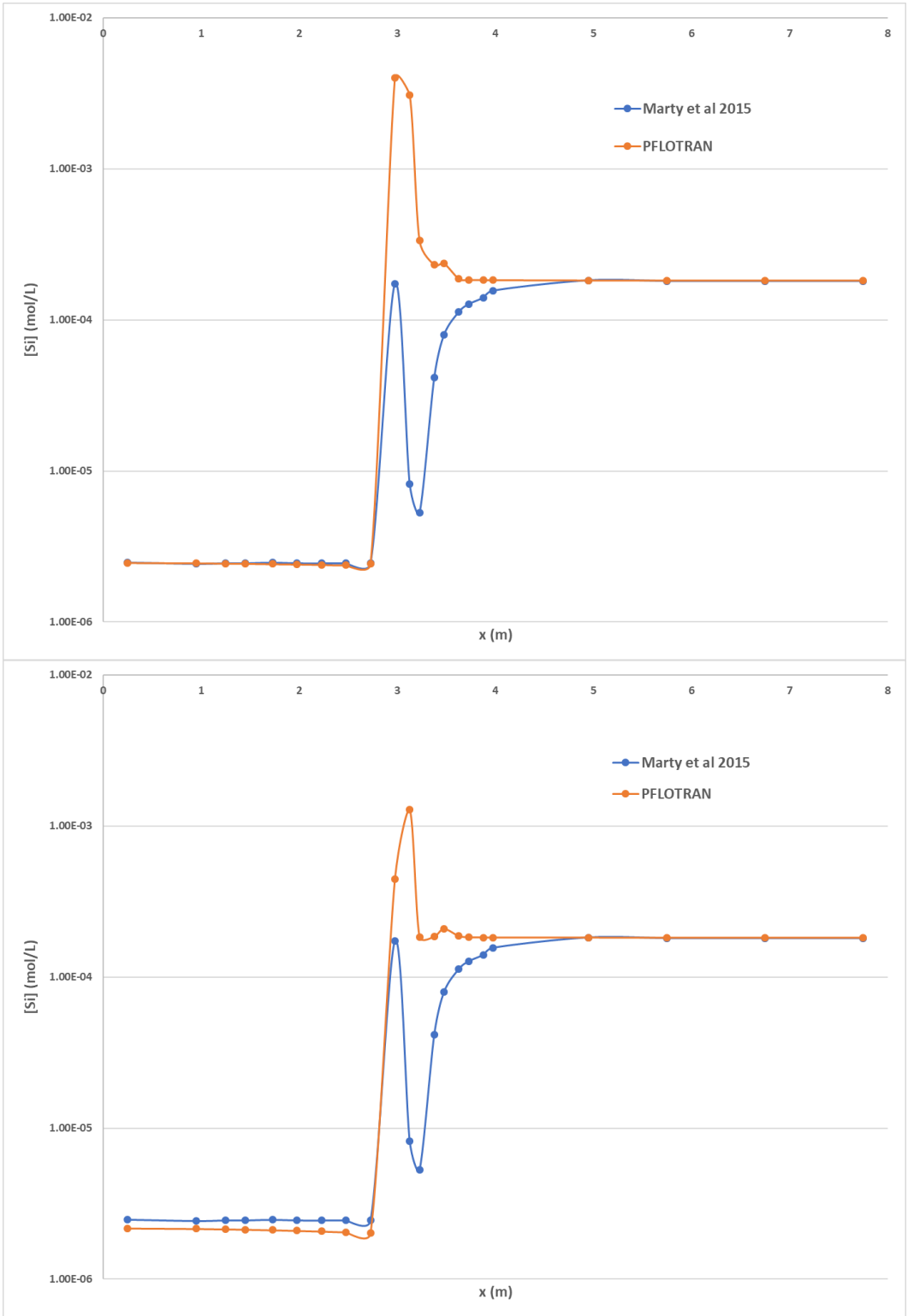

Figure 3-4. Si concentration in the case with (above) and without (below) ettringite precipitation in the cement.

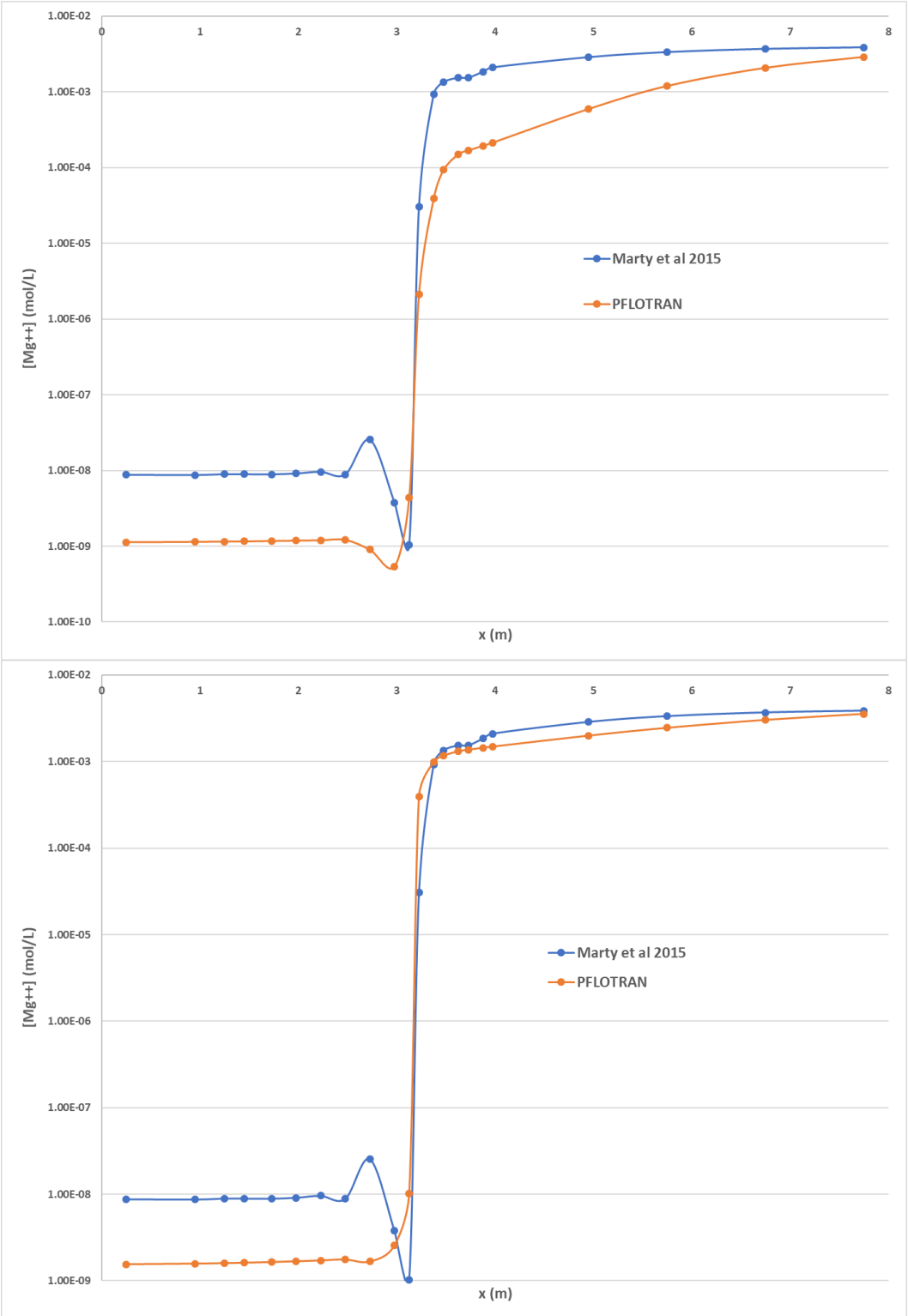

Figure 3-5. Mg^{++} concentration in the case with (above) and without (below) ettringite precipitation in the cement.

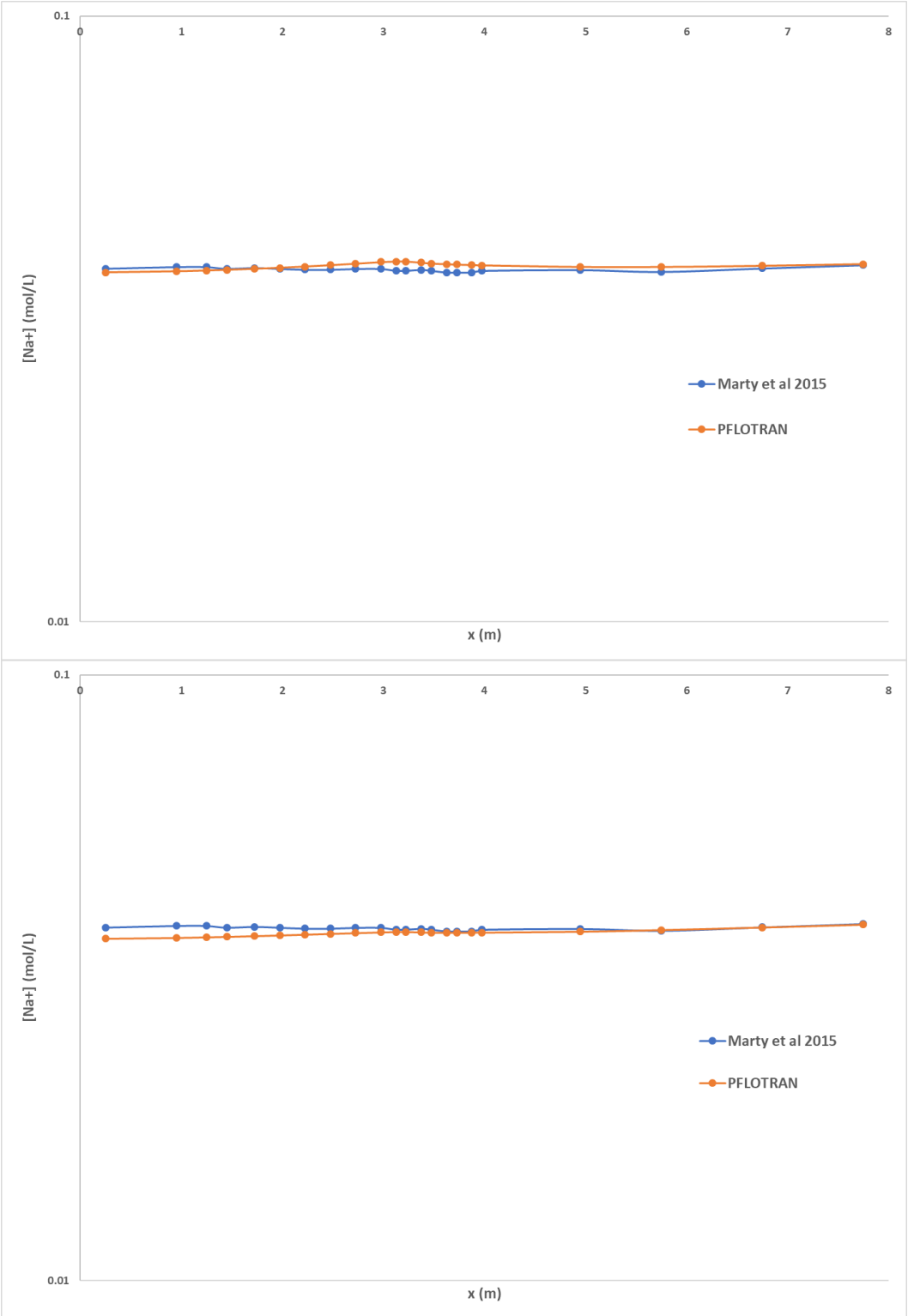

Figure 3-6. Na^+ concentration in the case with (above) and without (below) ettringite precipitation in the cement.

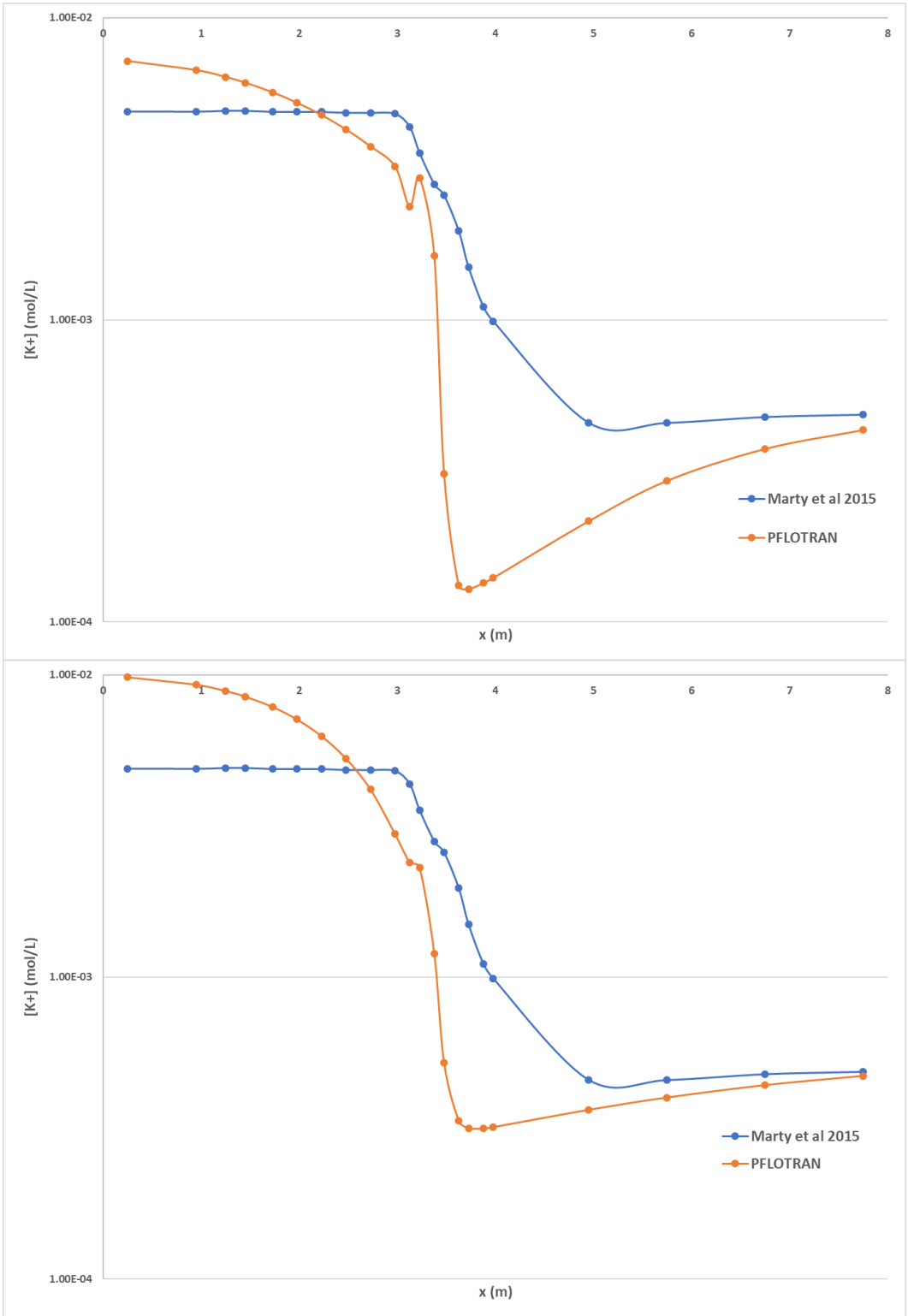

Figure 3-7. K^+ concentration in the case with (above) and without (below) ettringite precipitation in the cement.

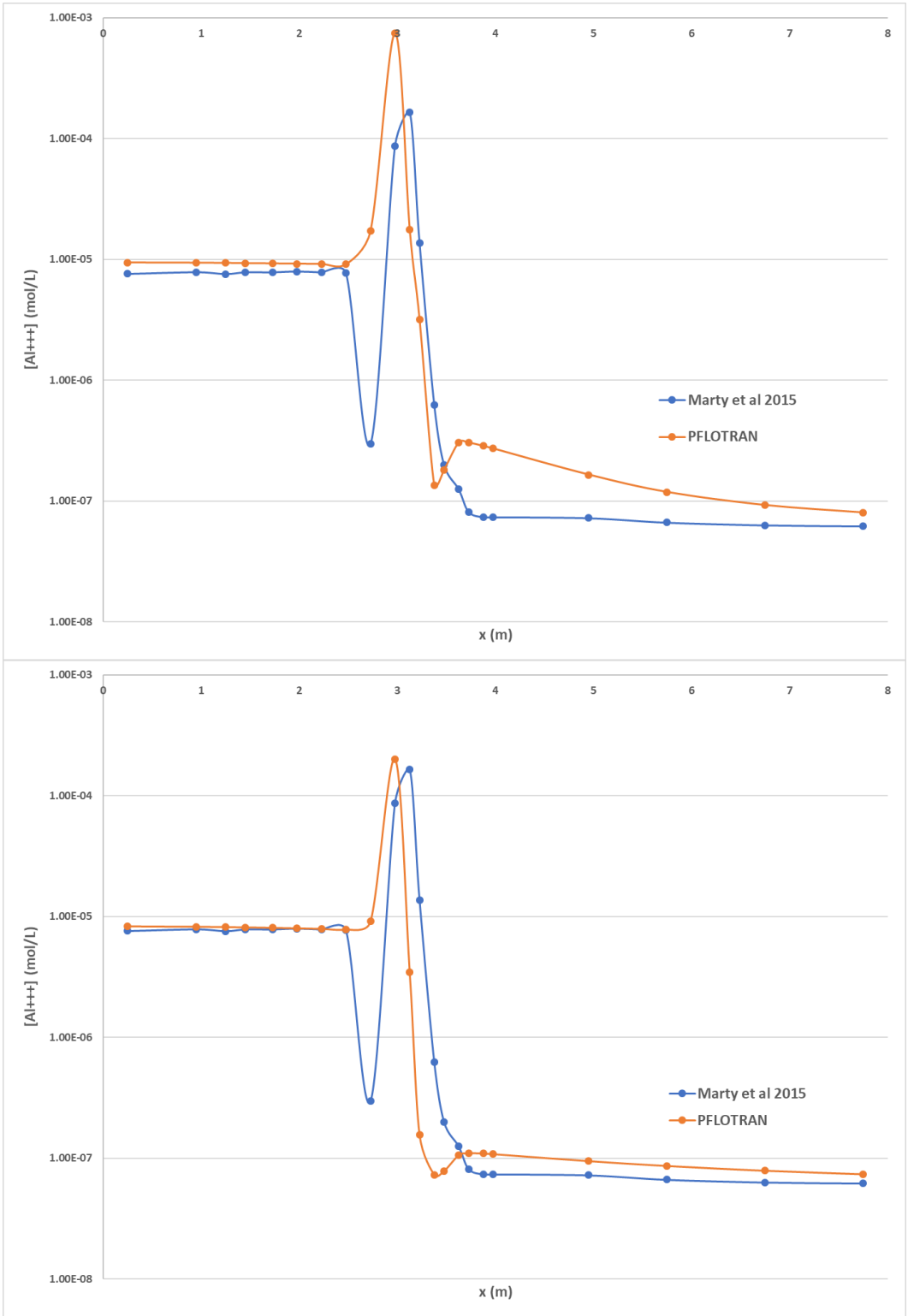

Figure 3-8. Al^{+++} concentration in the case with (above) and without (below) ettringite precipitation in the cement.

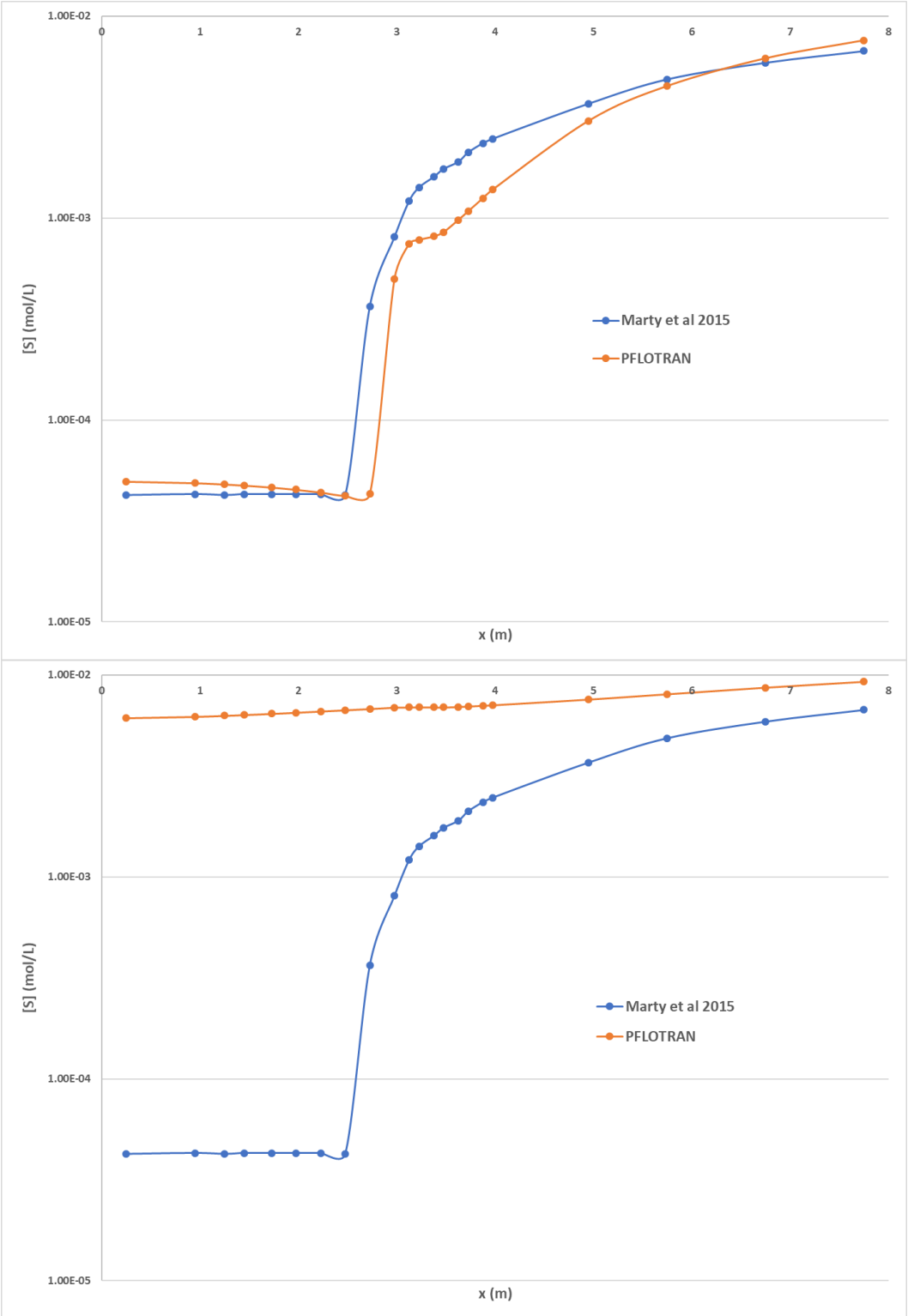

Figure 3-9. S concentration in the case with (above) and without (below) ettringite precipitation in the cement.

4. BARRIER MATRIX INTERACTIONS WITH GEOLOGIC STRATA IN THE SUBSURFACE OF THE YAMIN PLATEAU, NORTHERN NEGEV, ISRAEL

4.1 Introduction

These activities are focused on providing characterization of the long-term performance of interfaces between cementitious materials (CEM I and low pH cement) with carbonate geologic strata (i.e., marl, limestone, chalk, oil shale, phosphate rock) of the northern Negev, Israel with respect to primary phases constituents and diffusive transport of indicator surrogates of radionuclides. These cases will serve as experimental validation cases for the modelling tools discussed in the previous chapter (Chapter 3), including a comparative modeling study between PFLOTRAN and LeachXS/ORCHESTRA.

4.1.1 OBJECTIVES

The work described in this chapter has two specific objectives:

1. Use laboratory experiments to characterize the reactions and transport of primary matrix constituents and indicator surrogates of radionuclides at the interface between carbonate rock types and cementitious barriers.

2. Demonstrate multiphase diffusion-reactive transport models for parameter estimation and to simulate long-term interactions considering potential future disposal in different Negev geologic formations.

4.1.2 SIGNIFICANCE

The significance of the work described in this chapter is as follows:

- In deep geological disposal sites for radioactive waste, interfaces between cementitious materials, used either as engineered structures or as wasteforms, and host-rock are often found.

- As carbonate rocks have not been previously considered as host rocks for a deep geological repository of nuclear waste, their interaction with cement phases has not been studied extensively.

- Such interfaces might lead to chemical and structural alteration of both the cement and the rock. In the case of carbonate rocks, carbonation of the cement hydration products (e.g. portlandite, C-S-H, and ettringite) leads to pH decrease in the paste. Portlandite carbonation results in subsequent decalcification of C-S-H that leads to changes in the cement strength and may lead to structural failure. Furthermore, the mobility of trace constituents (e.g. radionuclides) may increase in response to changes in pH, porosity, and mineralogical gradients.

- The results of the project may be used for design and performance assessment (PA) of deep geological repository of nuclear waste in a typical carbonate rocks.

4.2 Materials and Methods

Samples were obtained from geologic strata of the Yamin Plateau in the Negev Desert in southern Israel. A set of leaching tests have been completed and several more are underway. This includes in-depth chemical characterization of solution and solid phase compositions. This information is then used in

computational modelling of the leaching tests. Results from the first round of leaching tests and simulations of the tests are shown below in Section 4.2.6.

4.2.1 Samples and materials characterization

- Rock Samples included: limestone, chalk, marl, oil shale, high organic material phosphorite and low organic material phosphorite.
- Cement samples included: CEM I (OPC paste) and low pH cement paste.

  Cements are doped with the following dopants at concentration of 500 mg/kg: uranyl nitrate, cerium (III) chloride, sodium chromate, and lithium bromide.
- Analyses completed on rock and cement samples: **1. Solid characterization:** Whole rock XRD, Clay XRD, TGA, Insoluble residue, Total content ($LiBO_2$ fusion), total organic content (TOC), microstructure (SEM-BSE, SEM-EDS) **2. Petrophysical:** specific surface area, porosity, pore size distribution (MIP, BET) **3. Liquid characterization:** pH, major and trace inorganic constituents (by ICP-MS, ICP-OES, IC), dissolved organic and inorganic carbon (DOC, DIC)

4.2.2 Experimental program

- Leaching analysis: **1. EPA 1313**, pH dependence leaching test (examples for limestone and OPC paste in Figures 1 and 2) and **2. EPA 1315**, semi-dynamic transport tests (example for limestone in Figure 3) tests were completed for both rock and cement samples.
- Cement-Rock interface casting – A methodology for running the experiments was developed and implemented during 2019 (Figure 4).
- 12 different types (2 types of cement and 6 types of carbonate rocks) of interface experiments will be cast before October 2019:

OPC paste/limestone	Low pH cement/limestone
OPC paste/chalk	Low pH cement /chalk
OPC paste/marl	Low pH cement /marl
OPC paste/oil shale	Low pH cement /oil shale
OPC paste/high organic phosphorite	Low pH cement /high organic phosphorite
OPC paste/low organic phosphorite	Low pH cement /low organic phosphorite

4.2.3 Simulations – database and code enhancements

- LeachXS/ORCHESTRA platform was used for developing a geochemical reactive transport model that considers: mass transport, cement chemistry, geochemical speciation, and multi-ionic diffusion
- Implementation of a new, most up-to-date, thermodynamic database for chemical reaction of cementitious materials CEMDATA18(Lothenbach, et al. 2019) in ORCHESTRA has been completed.
- The thermodynamic databases that are being used for simulations, CEMDATA18 and MinteqV4 were adjusted from 25 °C to the actual temperature of the experimental data from the lab - 30 °C and to 15, 20 and 35 °C.

- Conceptual model for interface experiments and Multi ionic diffusion model – were developed and implemented.
- The capability to use dissolution/precipitation kinetics in the simulations code was developed and integrated.

4.2.4 Simulations – Calibration of mineral sets and reactive phases

- Calibration of mineral reaction sets for rocks samples and low pH cement completed for limestone, marl, OPC paste and low pH cement (example for limestone and OPC paste in figures 1 and 2).

4.2.5 Reactive transport simulations

- The samples tortuosity was calibrated based on 1315 tests using LiBr as ingress tracer for rock and cement samples (Figure 3 – example for limestone). Tortuosity was found by repetitive simulations of the experiment with different tortuosity values until finding the minimum residual between the measured Li and Br concentration and the model prediction.
- Validation of the mineral reaction set and tortuosity calibration was done by comparing the independent data of measured pH and calcium concentrations during EPA 1315 test to the predication of the model (dashed blue line figure 3).

4.2.6 Rock/cement interface simulations

- **Chemical properties** that were measured (i.e. experimental data from EPA1313) and calibrated (i.e. calibrated mineral reaction set) were used as input for the chemical properties of the interface model.
- The union of calibrated mineral reaction sets of each pair of rock and cement was used to describe the system. Independent simulations of each material with the union of mineral reaction sets were done to verify that this method didn't change the simulated mineralogy of each of the parent materials.
- **Physical properties** that were measured (porosity) and calibrated (tortuosity) were used as input for the physical properties of the interface model.
- **Preliminary results – Figure 4-5** shows Ca and Si profiles distribution within different mineralogical phases along the limestone/OPC paste interface. 5 years were simulated. Two main findings were observed in simulations:
    - Carbonation rates (of cement) are dependent on dissolved carbonate flux from carbonate rocks to cement. The thickness of carbonated cement is proportional to the ratio between porosity to tortuosity within the cement.
    - Altered rock thickness layer is related to OH^- (alkaline pH) flux from cement to the rocks and to solubility constants of the solid phases ($CdSiO_3$, CNASH solid solution, Co_2SiO_4, Ni_2SiO_4, Willemite).

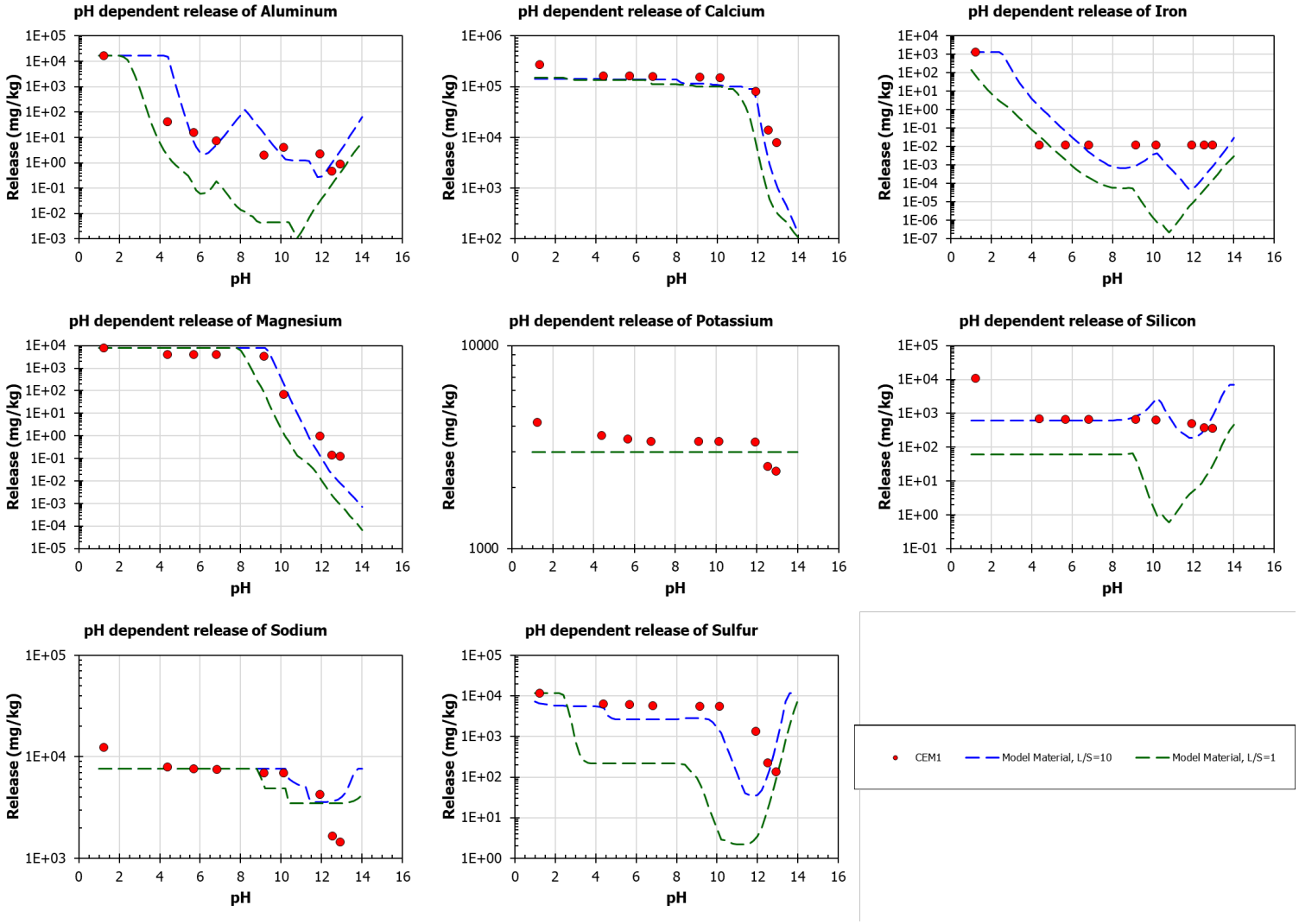

Figure 4-1. CEM1. Results of mineral reaction set calibration based on experimental results derived from EPA 1313. The red dots are the experimental results of EPA 1313 with CEM1 sample. The dashed blue and green lines are the prediction of the experimental results using the calibrated mineral reaction set L/S ratio of 10 and 1 respectively.

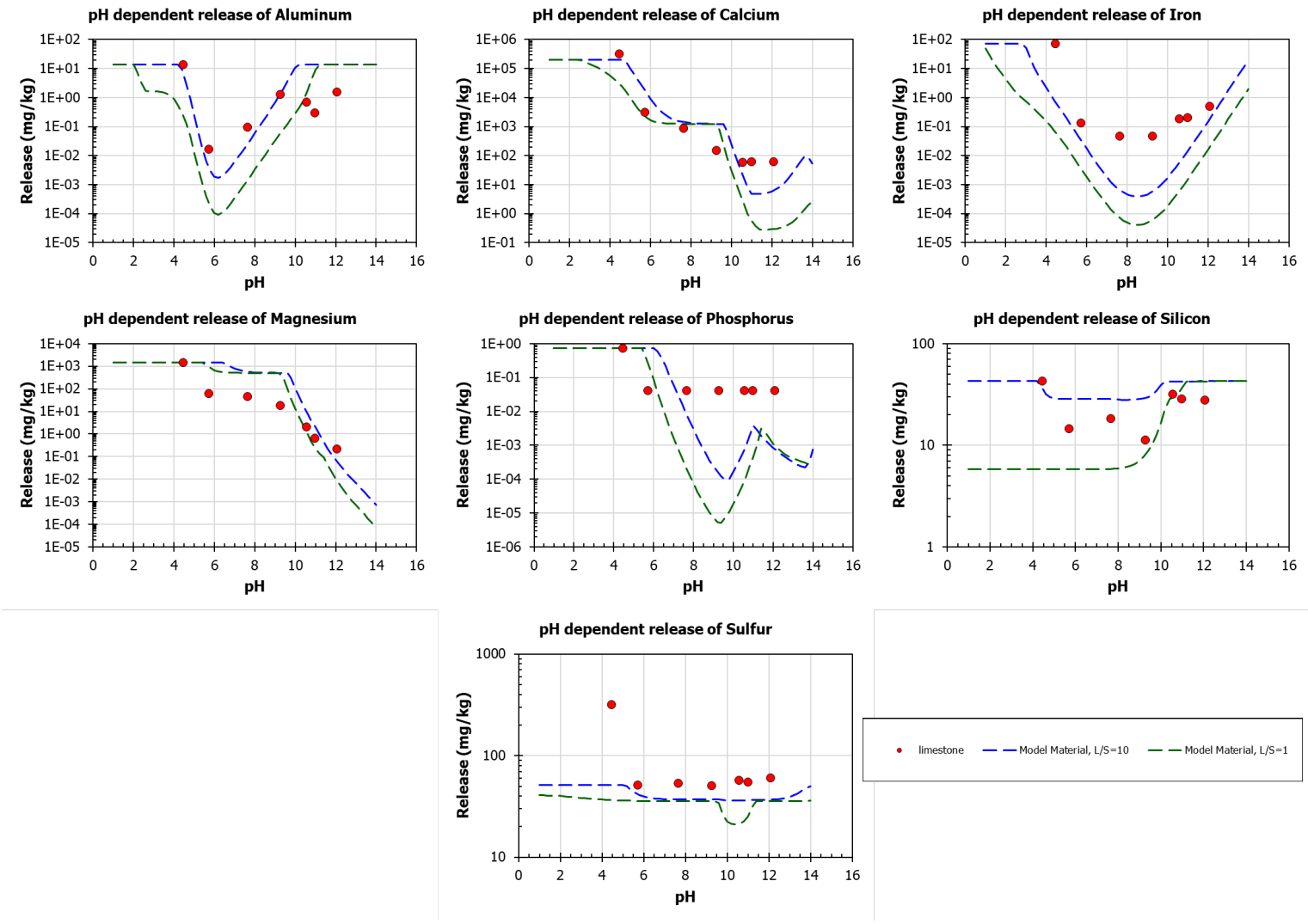

Figure 4-2. Limestone. Results of mineral reaction set calibration based on experimental results derived from EPA 1313. The red dots are the experimental results of EPA 1313 with CEM1 sample. The dashed blue and green lines are the prediction of the experimental results using the calibrated mineral reaction set at L/S of 10 and 1 respectively.

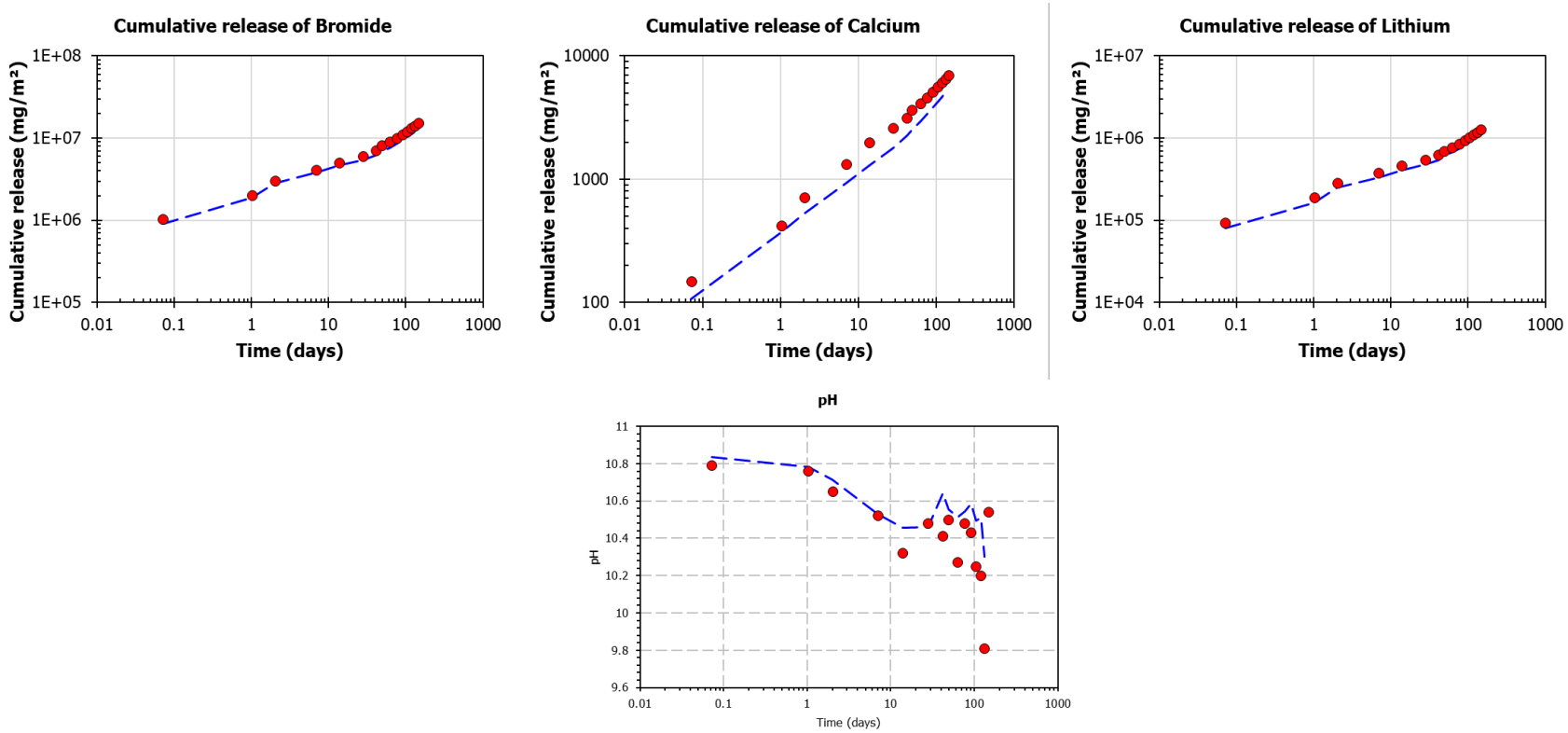

Figure 4-3. Tortuosity calibration for limestone rock based on experimental results derived from EPA 1315. The red dots are the experimental results of EPA 1315 with Limestone sample. The dashed blue line is the prediction of the experimental results using the calibrated mineral reaction set and the chemical composition and contact duration of refreshment solutions with the sample.

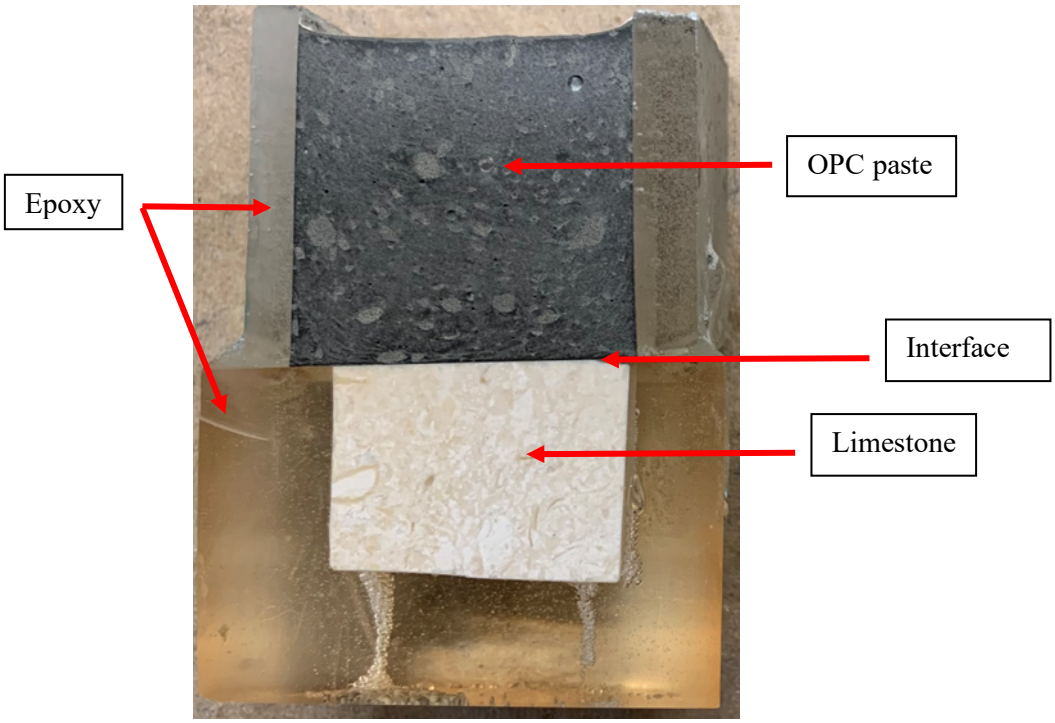

Figure 4-4. Example for Interface experiment: limestone-OPC paste.

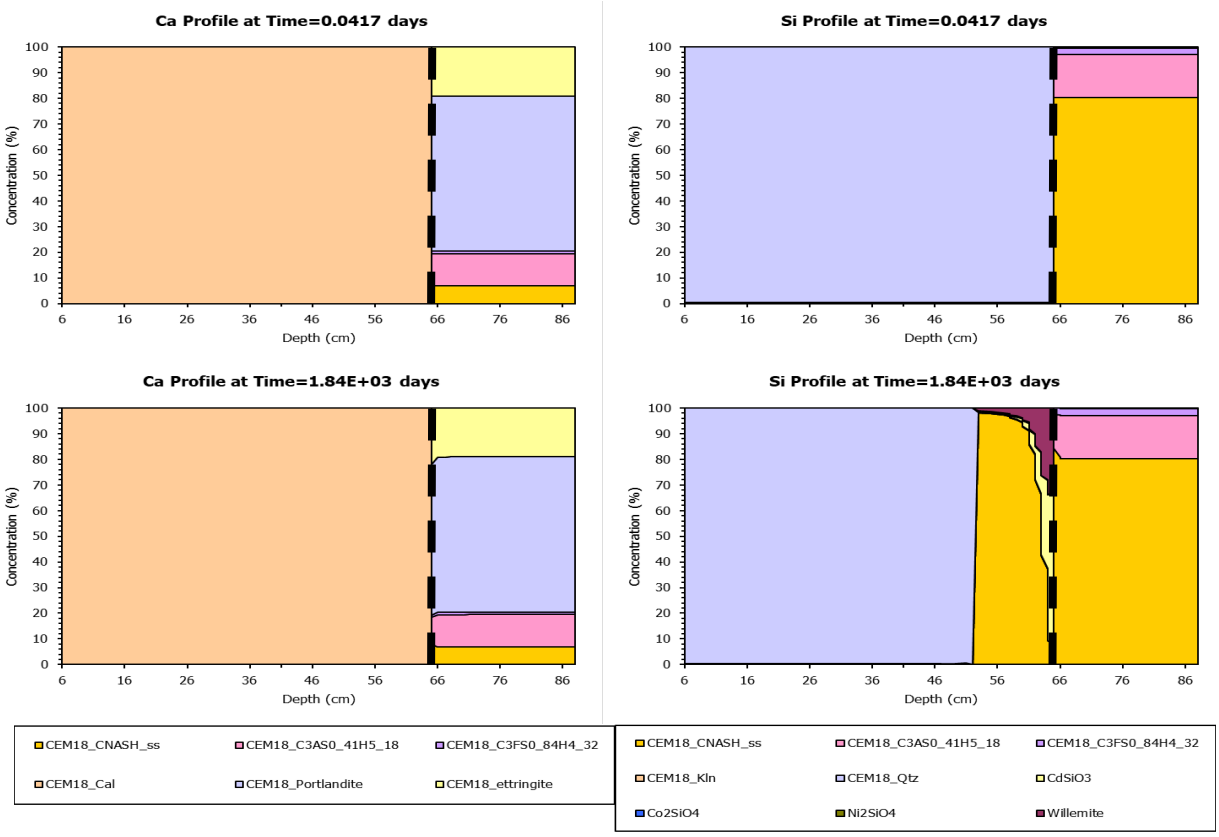

Figure 4-5. Results of limestone-OPC paste cement interface simulation. Ca and Si profiles distribution within different mineralogical phases along the limestone/OPC paste interface. The upper profiles show the distribution after simulated 0.04 day and the lower profiles show after simulated 5 years (about 1840 days). Dashed black line represents the original position of the interface.

REFERENCES

Adams, B.M., L.E. Bauman, W.J. Bohnhoff, K.R. Dalbey, M.S. Ebeida, J.P. Eddy, M.S. Eldred, P.D. Hough, K.T. Hu, J.D. Jakeman, J.A. Stephens, L.P. Swiler, D.M. Vigil, and T.M. Wildey, Dakota, A Multilevel Parallel Object-Oriented Framework for Design Optimization, Parameter Estimation, Uncertainty Quantification, and Sensitivity Analysis: Version 6.0 User's Manual (SAND2014-4633), 2014, Sandia National Laboratories: Albuquerque, New Mexico.

Berner, U., Kulik, D. A., and Kosakowski, G., 2013, Geochemical impact of a low-pH cement liner on the near field of a repository for spent fuel and high-level radioactive waste: Physics and Chemistry of the Earth, Parts A/B/C, v. 64, no. 0, p. 46-56.

Blanc, P., Lassin, A., Piantone, P., Azaroual, M., Jacquemet, N., Fabbri, A., and Gaucher, A., 2012, Thermoddem: A geochemical database focused on low temperature water/rock interactions and waste materials: Applied Geochemistry, v. 27, p. 2107-2116.

Blanc, P., Piantone, P., Lassin, A., and Burnol, A., 2006, Thermochimie : Sélection de constantes thermodynamiques pour les éléments majeurs, le plomb et le cadmium, Rapport final BRGM/RP-54902-FR: France, BRGM, p. 157.

Gaboreau, S., Lerouge, C., Dewonck, S., Linard, Y., Bourbon, X., Fialips, C. I., Mazurier, A., Pret, D., Borschneck, D., Montouillout, V., Gaucher, E. C., and Claret, F., 2012, In-Situ Interaction of Cement Paste and Shotcrete with Claystones in a Deep Disposal Context: American Journal of Science, v. 312, no. 3, p. 314-356.

Kosakowski, G., and Berner, U., 2013, The evolution of clay rock/cement interfaces in a cementitious repository for low- and intermediate level radioactive waste: Physics and Chemistry of the Earth, v. 64, p. 65-86.

Lichtner, P. C., Hammond, G. E., Lu, C., Karra, S., Bisht, G., Andre, B., Mills, R. T., and Kumar, J., 2013, PFLOTRAN User Manual: http://www.pflotran.org.

Lothenbach, B., Kulik, D.A., Matschei, T., Balonis, M., Baquerizo, L., Dilnesa, B., Miron, G.D. and Myers, R.J. (2019) Cemdata18: A chemical thermodynamic database for hydrated Portland cements and alkali-activated materials. Cement and Concrete Research 115, 472-506.

Mariner, P.E., W.P. Gardner, G.E. Hammond, D. Sevougian, and E. Stein, Application of Generic Disposal System Models (FCRD-UFD-2015-000126), 2015, Sandia National Laboratories: Albuquerque, NM.

Marty, N. C., Bildstein, O., Blanc, P., Claret, F., Cochepin, B., Gaucher, E. C., Jacques, D., Lartigue, J.-E., Liu, S., and Mayer, K. U., 2015, Benchmarks for multicomponent reactive transport across a cement/clay interface: Computational Geosciences, p. 1-19.

Soler, J. M., 2012, High-pH plume from low-alkali-cement fracture grouting: Reactive transport modeling and comparison with pH monitoring at ONKALO (Finland): Applied Geochemistry, v. 27, no. 10, p. 2096-2106.

Soler, J. M., and Mader, U. K., 2010, Cement-rock interaction: Infiltration of a high-pH solution into a fractured granite core: Geologica Acta, v. 8, no. 3, p. 221-233.